

Oxidative stress-associated rise of hepatic protein glycation increases inflammatory liver injury in uncoupling protein-2 deficient mice

Angela Kuhla¹, Christina Hettwer¹, Michael D Menger² and Brigitte Vollmar¹

Mitochondrial dysfunction seems to be intrinsically involved in the pathogenesis of multiple organ failure because of enhanced production of reactive oxygen species and induction of oxidative damage. Chronic oxidative stress in turn causes an accumulation of advanced glycation end products (AGEs). To investigate whether mitochondrial dysfunction-associated oxidative stress leads to increased formation and accumulation of AGE, we studied hepatic glycation in uncoupling protein-2 (UCP2^{-/-}) knockout mice. Using the galactosamine/lipopolysaccharide (G/L)-induced liver injury model, we further tested the hypothesis that a mitochondrial dysfunction-associated increase of hepatic glycation is causative for increased liver injury. Under baseline conditions, UCP2^{-/-} mice showed higher malondialdehyde levels and reduced glutathione/glutathione disulfide ratios as well as significantly higher hepatic levels of AGE and hepatic expression of receptor for AGE (RAGE) when compared with UCP2^{+/+} mice, indicative for increased oxidative stress and hepatic glycation. Further, livers of G/L-challenged UCP2^{-/-} mice revealed significantly more pronounced tissue injury and were found to express higher levels of AGE and RAGE compared with wild-type mice. Functional blockade of RAGE by application of recombinant RAGE significantly diminished liver damage particularly in UCP2^{-/-} mice. This in turn increased survival from 30% in UCP2^{+/+} mice to 50% in UCP2^{-/-} mice. In summary, we show for the first time that mitochondrial dysfunction-associated oxidative stress enhances hepatic protein glycation, which aggravates inflammation-induced liver injury. Targeting the AGE/RAGE interaction by the blockade of RAGE might be of therapeutic value for the oxidative stress-exposed liver.

Laboratory Investigation (2010) 90, 1189–1198; doi:10.1038/labinvest.2010.84; published online 5 April 2010

KEYWORDS: mitochondrial dysfunction; AGEs; receptor for AGEs; inflammation; survival; liver injury

Mitochondria are thought to have a key role in the process of aging and in the etiology and progression of a number of age-related disorders. It has been proposed that mitochondria are the biological clock, because mitochondrial dysfunction leads to an overproduction of reactive oxygen species (ROS) and thus 'chronic' oxidative stress.^{1,2} As a by-product of oxidative phosphorylation in the mitochondria, superoxide anion is produced within the mitochondria. The production of superoxide increases with overwhelming fuel supply because of a limited electron transport by hyperpolarization of the inner mitochondrial membrane or with the functional impairment of one or more electron transport complexes.³ Uncoupling proteins are embedded in the inner mitochondrial membranes and belong to the family of mitochondrial ion transporters. Uncoupling protein-2 (UCP2) has been

proposed to limit the production of ROS by decreasing the mitochondrial membrane potential.^{4–6} In line with this, overexpression of UCP2 in various cell types exerted cytoprotection by limited ROS formation.^{7,8} Conversely, a defect in UCP2 expression or an inhibition of UCP2 function result in increased ROS generation, as illustrated by various *in vitro* and *in vivo* experiments.^{9,10}

Besides increased oxidative stress, protein glycation with accumulation of advanced glycation end products (AGE) represents a main mechanism involved in biological aging. AGE are heterogeneous compounds resulting from non-enzymatic, irreversible glycation/glycooxidation of proteins and other biomolecules (also called Maillard reaction).^{11,12} AGE were originally characterized by a yellow-brown fluorescent color and the ability to form crosslinks with and

¹Institute for Experimental Surgery, University of Rostock, Rostock, Germany and ²Institute for Clinical & Experimental Surgery, University of Saarland, Homburg/Saar, Germany

Correspondence: Dr B Vollmar, MD, Institute for Experimental Surgery, University of Rostock, Schillingallee 69a, 18057 Rostock, Germany.
E-mail: brigitte.vollmar@med.uni-rostock.de

Received 27 December 2009; revised 9 February 2010; accepted 10 February 2010

between amino groups.^{13,14} During normal aging and in particular in age-related diseases high-modified nonsoluble AGE are formed, which are resistant to proteasomal degradation. This leads to an increased accumulation of AGE in various tissues.^{15–17} AGE precursor compounds, such as methylglyoxal and glyoxal, are detoxified by the cellular glyoxalase system, consisting of glyoxalases I and II that convert AGE precursor compounds to lactate and finally to pyruvate.^{18,19} In contrast to the metabolism of low-modified AGE, high-modified AGE such as AGE-BSA are eliminated by liver sinusoidal endothelial cells and Kupffer cells through scavenger receptor-mediated endocytosis.²⁰ The capacity of AGE endocytosis is found to be reduced in aging livers, resulting in spillover into the systemic circulation and extrahepatic deposition of these waste macromolecules.²¹

The receptor for AGEs (RAGEs), a member of the immunoglobulin superfamily of cell-surface molecules, is a multiligand-binding receptor with an extracellular, transmembranal and cytosolic domain.^{22–24} Interaction of RAGE with diverse ligands was demonstrated to be involved in distinct developmental and pathological processes.²⁵ Binding of AGE to RAGE results in generation of intracellular oxidative stress and, subsequently, in activation of transcription factors such as NF- κ B,²⁶ leading to an enhanced inflammatory response and local tissue injury.²⁷ However, a truncated isoform of RAGE, that is, soluble RAGE (sRAGE) and an endogenous secretory RAGE, spanning the extracellular ligand-binding domain, have been reported to exert potent anti-inflammatory properties by acting as a decoy for RAGE ligands.²⁸

In this study, we have examined the liver function of UCP2 $-/-$ mice and their wild-type littermates under both baseline conditions and on an inflammatory stimulus and assumed that mitochondrial dysfunction in UCP2 $-/-$ mice enhanced oxidative stress. On the basis of this, we hypothesized that UCP2 $-/-$ mice present with increased formation and accumulation of AGE, which in turn contribute to an increased extent of hepatic injury. As a common experimental approach to study acute liver injury, galactosamine/lipopolysaccharide (G/L) administration was used. Galactosamine, an amino sugar, is exclusively metabolized in hepatocytes, leading to a selective depletion of uridine nucleotides.²⁹ This UTP depletion causes transcriptional inhibition and is considered to be responsible for the development of sensitization of the liver as main target organ to low lipopolysaccharide doses.²⁹ To provide final evidence that AGE/RAGE signaling is critically important in mediating liver injury, we applied rRAGE for blockade of the AGE/RAGE interaction and studied the efficacy of this emerging therapeutic agent in preventing G/L-induced liver dysfunction and failure.

MATERIALS AND METHODS

Animal Model

UCP2 $-/-$ mice were generated, as previously published³⁰ and were kept on the C57BL/6 background. For the

experiments, female wild-type littermates (UCP2 +/+) and knockout mice (UCP2 $-/-$) (generously provided by Daniel Ricquier and Bruno Miroux, CNRS UPR 9078, Medical Faculty Necker-Enfants-Malades, Paris, France) were used at 6–8 weeks of age with a body weight (BW) of \sim 20 g. Animals were kept on water and standard laboratory chow *ad libitum*. All animals received humane care according to the German legislation on protection of animals and the Guide for the Care and Use of Laboratory Animals (NIH publication 86–23, revised 1985).

G/L-Induced Liver Injury and Experimental Groups

For induction of acute liver failure, mice ($n=14$) were injected with galactosamine (G, 720 mg/kg BW i.p.; Sigma-Aldrich, Taufkirchen, Germany) and lipopolysaccharide (L, 10 μ g per kg BW i.p., *Escherichia coli* serotype 0128:B12; Sigma-Aldrich)^{31,32} and were studied 6 h later. Time-matched sham-treated animals with application of equivalent volumes of 0.9% saline were performed and designated as sham ($n=14$).

To verify the contribution of AGE/RAGE interaction in G/L-induced acute liver failure, additional animals were pretreated with recombinant mouse RAGE (rRAGE) as previously described³³ (10 μ g i.p., R&D Systems, Wiesbaden-Nordenstadt, Germany) or equivalent volumes of 0.9% saline 12 h before exposure to G/L. With a half time of 22 h for rRAGE,³⁴ this time point of application assures adequate action of rRAGE over the whole experimental time period.

Sampling and Assays

All animals were exsanguinated by puncture of the vena cava inferior for immediate separation of plasma, followed by harvest of liver tissue. Plasma aspartate aminotransferase (AST) and alanine aminotransferase (ALT) activities were measured spectrophotometrically as indicators for hepatocellular disintegration and necrosis.

Measurement of plasma malondialdehyde (MDA), serving as an indicator of lipid peroxidation and oxidative stress, was performed using the MDA-586 method according to the manufacturer's instructions (OxisResearch, Portland, OR, USA). Cellular redox environment in the plasma of UCP2 $-/-$ and UCP2 +/+ animals was assessed by measuring the ratio of glutathione (GSH) to glutathione disulfide (GSSG) using the GSH/GSSG-412 assay according to the manufacturer's instructions (OxisResearch).

Harvested liver tissue was processed for isolation of proteins. For this purpose, liver tissue was homogenized in lysis buffer (10 mM Tris pH 7.5, 10 mM NaCl, 0.1 mM EDTA, 0.5% Triton-X 100, 0.02% NaN₃ and 0.2 mM PMSF, protease inhibitor cocktail), incubated for 30 min on ice and centrifuged for 15 min at 10 000 g. Protein contents were assayed by bicinchoninic acid method (Pierce, Biotechnology) with BSA (Pierce, Biotechnology) as standard.

Assessment of Hepatic Concentration of sRAGE and Glyoxalase-I Activity

The concentration of sRAGE in liver extract was analyzed with a commercially available DuoSet enzyme-linked immunosorbent assay kit in accordance to the manufacturer's instructions (R&D Systems). Hepatic levels of sRAGE were calculated by dividing the total sRAGE concentration by the amount of total protein per microliter in the preparation.

The activity of glyoxalase-I in hepatic protein extracts was measured using the hemithioacetal of methylglyoxal as substrate according to the method of Allen *et al.*³⁵ Briefly, 2 μmol methylglyoxal and 2 μmol GSH each in sodium phosphate buffer (50 mM, pH 6.6, 995 μl) were preincubated at 37°C for 10 min to form the hemithioacetal. Protein extract of 5 μl was added and the increase in absorbance was measured at 240 nm using a spectrophotometer (Utrospec 3000, Pharmacia Biotech, Cambridge, UK). Glyoxalase-I activity was calculated by Beer-Lambert law with $\Delta\epsilon_{240} = 2.86 \text{ mM/cm}$ and considering dilution factor and rate of reaction per minute.³⁵ The specific activity of glyoxalase-I was calculated by dividing the total glyoxalase-I activity by amount of total protein per microliter in the preparation.

Western Blot Analysis of Hepatic AGE and RAGE/sRAGE

On 12% SDS gels, 40 μg protein was separated and transferred to a polyvinylidene difluoride membrane (Immobilon-P; Millipore, Eschborn, Germany). After blockade with 2% BSA (Santa Cruz Biotechnology, Santa Cruz, CA, USA), membranes were incubated overnight at 4°C with a mouse monoclonal anti-AGE³⁶ (1:500; clone No. 6D12, TransGenic, Kobe, Japan), and a rabbit polyclonal anti-RAGE/anti-sRAGE antibody³⁷ (1:500; Abcam, Cambridge, UK), followed by a secondary peroxidase-linked rabbit anti-mouse antibody (AGE; 1:10 000; Sigma) or a goat anti-rabbit antibody (RAGE/sRAGE; 1:5000; Santa Cruz Biotechnology). Protein expression was visualized by means of luminol-enhanced chemiluminescence (ECL plus; Amersham Pharmacia Biotech, Freiburg, Germany) and digitalized with ChemiDoc XRS System (Bio-Rad Laboratories, Munich, Germany). Signals were densitometrically assessed (Quantity One; Bio-Rad Laboratories) and normalized to the β -tubulin signals (rabbit polyclonal anti- β -tubulin antibody; 1:500; Santa Cruz Biotechnology).

Histology of Liver Tissue

For hematoxylin and eosin staining liver tissue was fixed in 4% phosphate-buffered formalin for 2–3 days and then embedded in paraffin. From the paraffin-embedded tissue blocks, 4 μm sections were put on glass slides and stained with hematoxylin and eosin. For histomorphometric analysis of necrotic tissue images of 20 random low-power fields ($\times 100$ magnification, Olympus BX 51, Hamburg, Germany) were acquired with a Color View II FW camera (Color View, Munich, Germany) and evaluated by means of an image analysis system (Adobe Photoshop, Adobe Systems,

Uxbridge, UK). The quotient of the focal necrosis surface to the total liver section area was assessed and given in percentage.

Survival Study

In a double-blinded manner, UCP2 $-/-$ ($n = 20$) and UCP2 $+/+$ ($n = 20$) animals were randomly numbered and exposed to either G/L or rRAGE and G/L, as mentioned above. Observation of death was carried out every 30 min for the first 12 h. The final survival rate was determined at 24 h after G/L exposure.

Statistical Analysis

All data are expressed as means \pm s.e.m. Statistical differences between strains under baseline conditions were determined using an unpaired Student's *t*-test. For statistical differences between either strains or treatment we used ANOVA, followed by post-hoc pairwise comparison tests for analysis. Data were considered significant if $P < 0.05$. Statistical analysis was carried out using the SigmaStat software package (Jandel Scientific, San Rafael, CA, USA).

RESULTS

Enhancement of Oxidative Stress is a Precondition for Glycation

To evaluate the potential impact of oxidative stress for glycation, we first determined the plasma MDA levels, the GSH to GSSG ratio and the glyoxalase-I activity in UCP2 $+/+$ and UCP2 $-/-$ mice (Figures 1a–c). We detected significantly higher lipid peroxidation (MDA) in UCP2 $-/-$ mice compared with UCP2 $+/+$ mice (Figure 1a). In confirmation of that, UCP2 $-/-$ mice revealed increased oxidative stress as indicated by an accumulation of GSSG and, thus, a significantly lower ratio of GSH to GSSG (Figure 1b). Furthermore, the activity of glyoxalase-I, indicating detoxification capacity of AGE precursor compounds, was significantly decreased in UCP2 $-/-$ mice when compared with UCP2 $+/+$ controls (Figure 1c).

Hepatic AGE and RAGE Levels are Increased in UCP2 $-/-$ Mice

To further examine whether the increased oxidative stress in UCP2 $-/-$ animals aggravates the glycation process, we determined the hepatic level of AGE. Western blot analysis of AGE showed multiple bands ranging from 12 to > 60 kDa, representing several AGE compounds.³⁸ We chose the 60 kDa band because the albumin-related AGEs with a molecular weight of about 66.000 g/mol are the most common AGE compounds. We could demonstrate that the UCP2 $-/-$ phenotype is associated with a significant increase of AGE in liver tissue when compared with UCP2 $+/+$ mice (Figure 2a). We further explored the expression of RAGE by using a polyclonal anti-RAGE antibody for western blot analysis (50 kDa) and could show significantly higher levels of RAGE in the livers of UCP2 $-/-$ mice (Figure 2b).

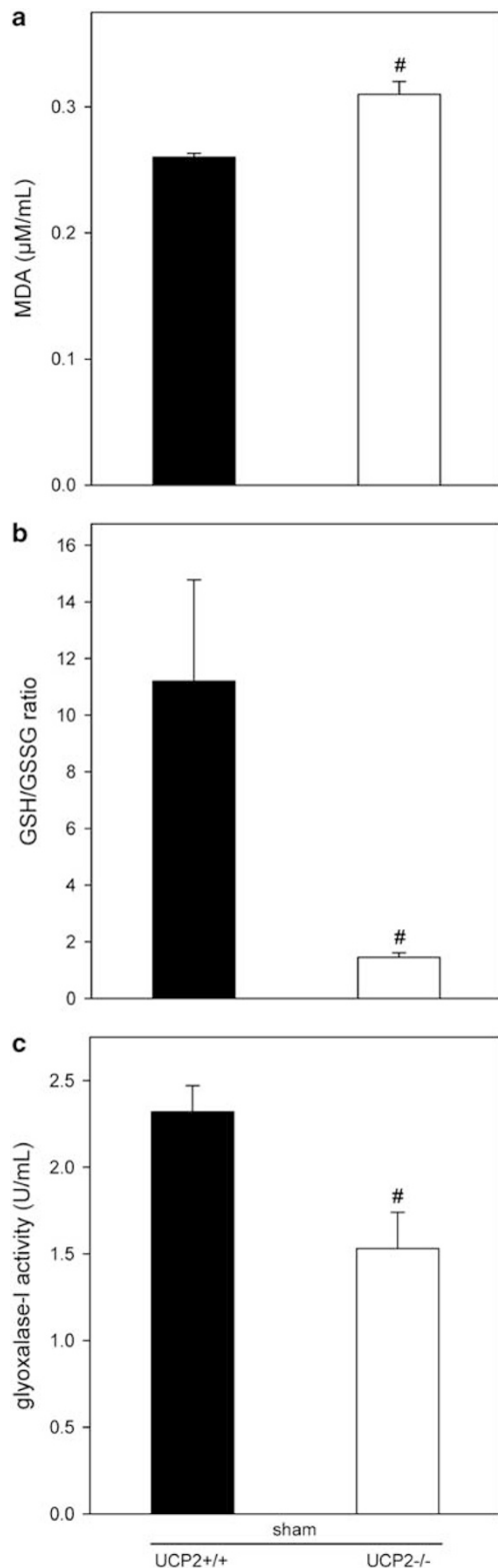


Figure 1 Analysis of plasma MDA (a), ratio of GSH to GSSG (b) and activity of glyoxalase-I (c) in sham-treated UCP2^{+/+} ($n=7$) and UCP2^{-/-} mice ($n=7$). Note the very low ratio of GSH to GSSG and the low activity of glyoxalase-I in UCP2^{-/-} mice. Values are given as means \pm s.e.m.; unpaired t-test: [#] $P < 0.05$ vs UCP2^{+/+} mice.

Hepatic sRAGE Expression and Concentration are Decreased in UCP2^{-/-} Mice

Owing to the fact that sRAGE acts as a decoy for RAGE ligands, we examined the expression of sRAGE by western blot (25 kDa band) and additionally evaluated the concentration of sRAGE in liver tissue extracts using an enzyme-linked immunosorbent assay. Both approaches revealed that the livers of UCP2^{-/-} mice exhibited markedly lower levels of sRAGE (Figures 3a and b).

G/L-Induced Liver Injury is Significantly Reduced by rRAGE Application in UCP2^{-/-} Mice

AST and ALT activities in plasma are given in Figure 4. G/L exposure induced marked liver injury, as indicated by significantly increased AST and ALT levels in both strains of mice when compared with sham-treated controls. It is interesting that transaminase release was significantly higher in the UCP2^{-/-} than in UCP2^{+/+} mice (Figures 4a and b), being well reflected by the notably more pronounced deterioration of morphology in UCP2^{-/-} liver specimen (Figure 5, mid panel). In support of this, quantitative analysis of hematoxylin and eosin histopathology of G/L-exposed livers exhibited focal necrosis in both mice strains, however, with almost twofold higher values in the UCP2^{-/-} mice (Figure 4c).

Along with the increased levels of AGE and RAGE as well as the pronounced liver injury, UCP2^{-/-} mice most benefited from the application of rRAGE. This is given by the remarkable reduction of AST and ALT levels from > 2000 U/L to ~ 600 U/L (Figures 4a and b) and by the substantial reduction of necrotic tissue area from 44 to 0.1% (Figures 4c and 5).

Hepatic AGE levels and RAGE expression are markedly increased by G/L exposure and significantly reduced by rRAGE application in UCP2^{-/-} mice. G/L-challenged livers of both mice strain showed a twofold increase of AGE level and a threefold increase of RAGE expression (Figures 6a and b). Further, pretreatment with rRAGE reduced AGE levels and RAGE expression in both G/L-exposed mouse strains. However, reduction was far more pronounced in UCP2^{-/-} animals (Figures 6a and b), as given by a 70% reduction of AGE level and a 86% decrease of RAGE expression compared with 20 and 50% in the respective wild-type animals.

rRAGE Application Increases Survival Rate in G/L-Challenged UCP2^{-/-} Mice

All animals survived the first 6 h after induction of G/L (Figures 7a and b), but died after 7 h and later. Despite the remarkable differences in oxidative stress and stress-related formation of glycation products between UCP2^{-/-} and UCP2^{+/+} animals, both strains of mice showed comparable survival rate with 20% at 24 h after G/L injection (Figures 7a and b). However, UCP2^{-/-} mice benefited from the administration of rRAGE before the G/L exposure and

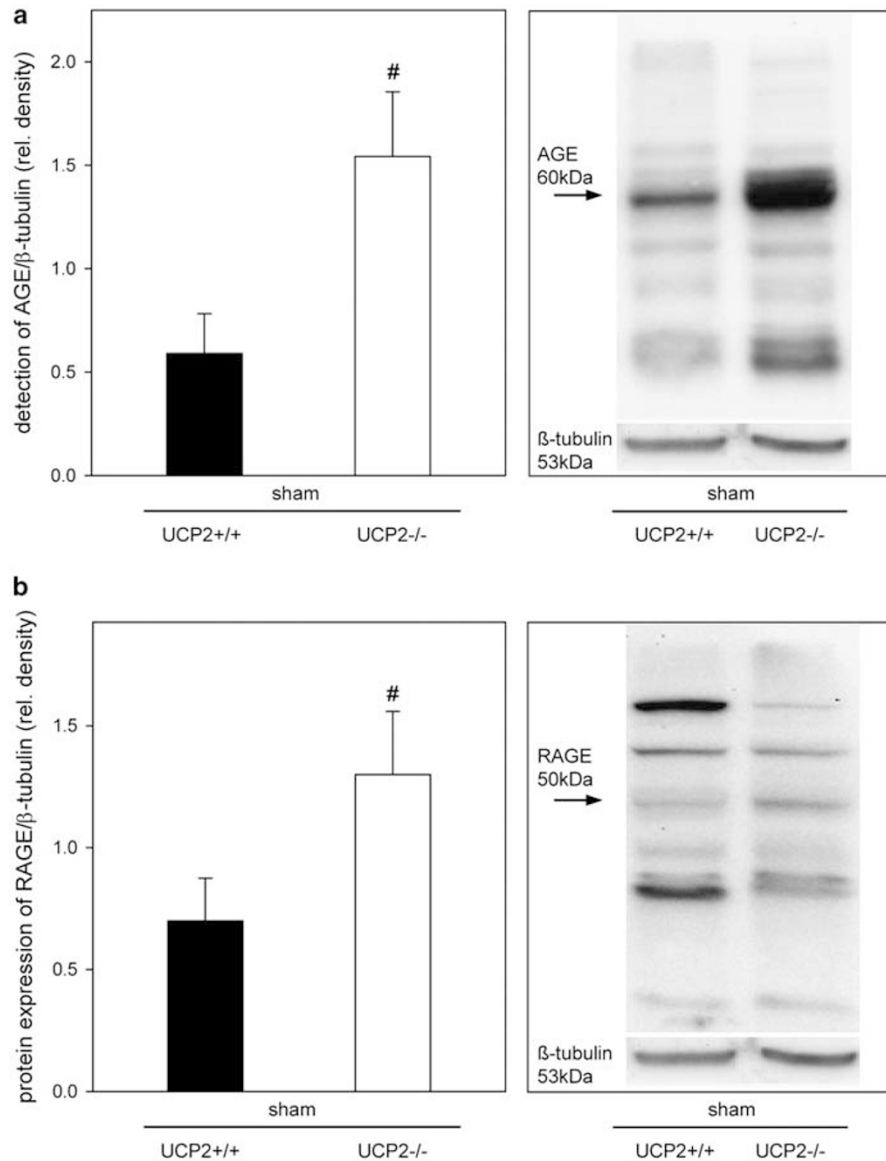


Figure 2 Densitometric analysis and representative western blots of AGE (60 kDa; **a**) and RAGE (50 kDa; **b**) in the livers of sham-treated UCP2^{+/+} ($n=7$) and UCP2^{-/-} mice ($n=7$). Signals were corrected with that of β -tubulin. Values are given as means \pm s.e.m.; unpaired t -test: $\#P<0.05$ vs UCP2^{+/+} mice.

showed an increased survival rate of 50% (Figure 7b), whereas UCP2^{+/+} mice still exhibited a survival rate of only 30% (Figure 7a).

DISCUSSION

The major findings of this study are that mitochondrial dysfunction is associated with (i) increased oxidative stress, (ii) hepatic AGE accumulation and increased RAGE expression, as well as (iii) enhanced hepatic vulnerability on G/L exposure. Interestingly, (iv) blockade of AGE/RAGE binding by rRAGE is capable of completely abolishing the mitochondrial dysfunction-associated increase in inflammatory injury.

It is well known that the mitochondria have a key role in cellular aging. They are major targets of free radical attack,^{2,39} which is responsible for a variety of age-related diseases.^{40,41} Further, there is accumulating evidence that during aging mitochondrial dysfunction occurs^{42,43} and that age-related oxidative stress and subsequently altered gene expression may cause a dysfunction of liver metabolism.²¹ This *in vivo* study now adds that mitochondrial dysfunction, as given by the deficiency for UCP2, elicits increased oxidative stress. We assumed that this may support the generation of nonenzymatically formed AGE, which are able to form crosslinks leading to accumulation of high-modified AGE. The latter are implicated in the pathogenesis of age-related diseases.^{44–46} Thus, our novel finding that mitochondrial

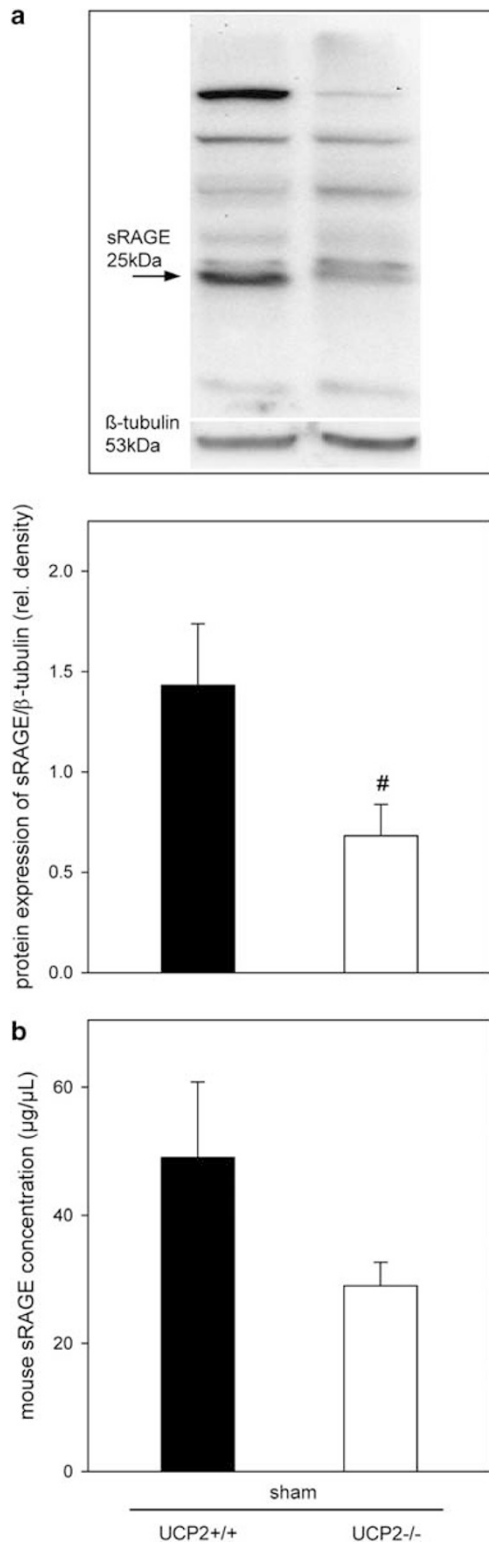


Figure 3 Representative western blot and densitometric analysis of sRAGE (25 kDa; **a**) and ELISA data of hepatic sRAGE release (**b**) in the livers of UCP2^{+/+} (n = 7) and UCP2^{-/-} animals (n = 7). Signals were corrected with that of β-tubulin. Values are given as means ± s.e.m.; unpaired *t*-test: #*P* < 0.05 vs UCP2^{+/+} mice.

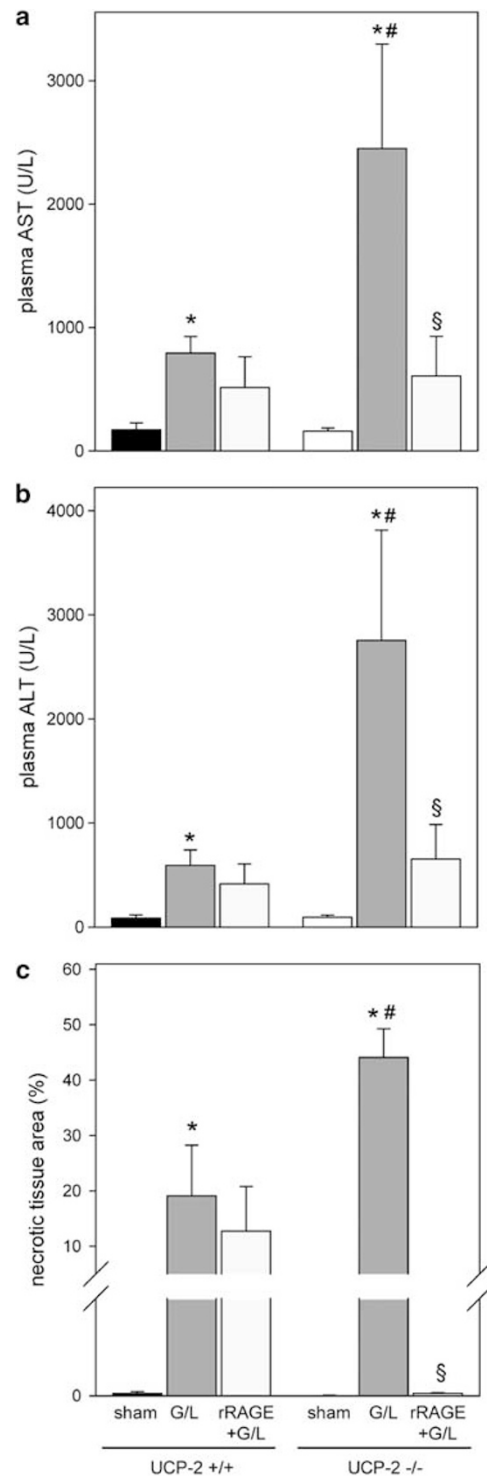


Figure 4 Plasma AST (**a**) and ALT activities (**b**), and histomorphometric analysis of necrosis (**c**) in UCP2^{+/+} (n = 21) and UCP2^{-/-} animals (n = 21). Animals were injected with either saline (sham; n = 14), G/L (720 mg/kg/10 μg/kg BW i.p.) (G/L; n = 14) or recombinant RAGE (10 μg i.p.; rRAGE + G/L; n = 14) at 12 h before G/L challenge. In all animals, analysis was carried out 6 h after G/L exposure. Note the high AST and ALT activities in G/L-exposed UCP2^{+/+}, but in particular in UCP2^{-/-} mice and the significant attenuation of injury after rRAGE pretreatment in the UCP2^{-/-} mice. Values are given as means ± s.e.m.; ANOVA, *post hoc* pairwise comparison tests: #*P* < 0.05 vs UCP2^{+/+}; **P* < 0.05 vs sham; §*P* < 0.05 vs G/L.

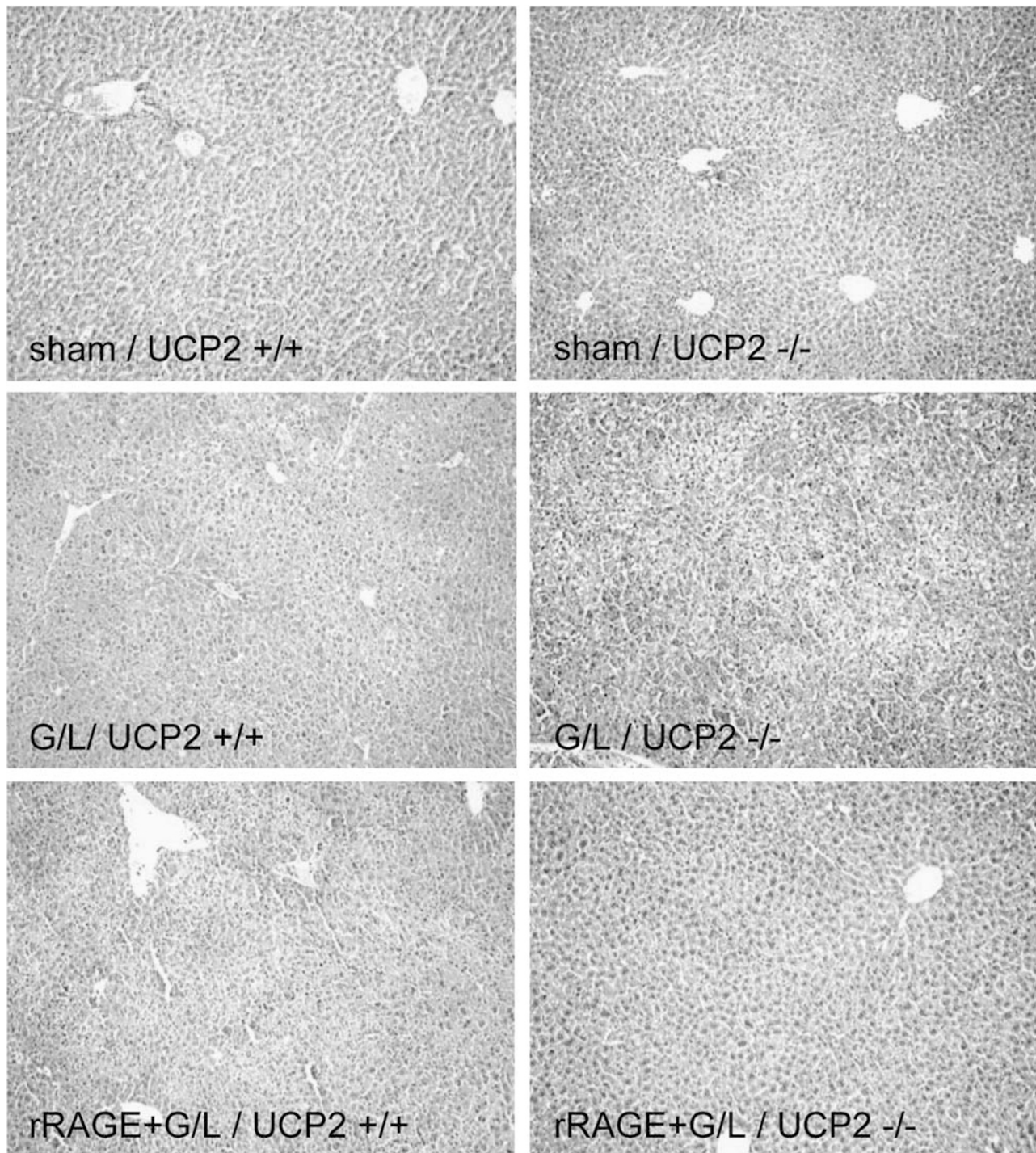


Figure 5 Representative hematoxylin and eosin-stained images of liver tissue (original magnification $\times 100$) in UCP2 $+/+$ ($n = 21$) and UCP2 $-/-$ animals ($n = 21$). Animals were injected with either saline (sham; $n = 14$), G/L (720 mg/kg/10 μ g/kg BW i.p.) (G/L; $n = 14$) or recombinant RAGE (10 μ g i.p.; rRAGE + G/L; $n = 14$) at 12 h before G/L challenge. In all animals, analysis was carried out 6 h after G/L exposure. Note the deterioration of hepatic morphology in G/L-exposed UCP2 $+/+$, but in particular in UCP2 $-/-$ mice and the significant attenuation of injury after rRAGE pretreatment in the UCP2 $-/-$ mice.

dysfunction-associated increase of oxidative stress enhances hepatic accumulation of high-modified AGE and hepatic vulnerability to inflammation is of potential value for the elaboration of new therapeutic strategies counteracting inflammatory liver injury. In this context, Sebeková *et al*⁴⁷

could demonstrate that patients with nonalcoholic liver cirrhosis exhibit markedly elevated *N*(ϵ)-carboxymethyl lysine-AGE. Such modifications of AGE cause alterations of protein structures, which become resistant to lysosomal degradation⁴⁸ and cause residual liver dysfunction.

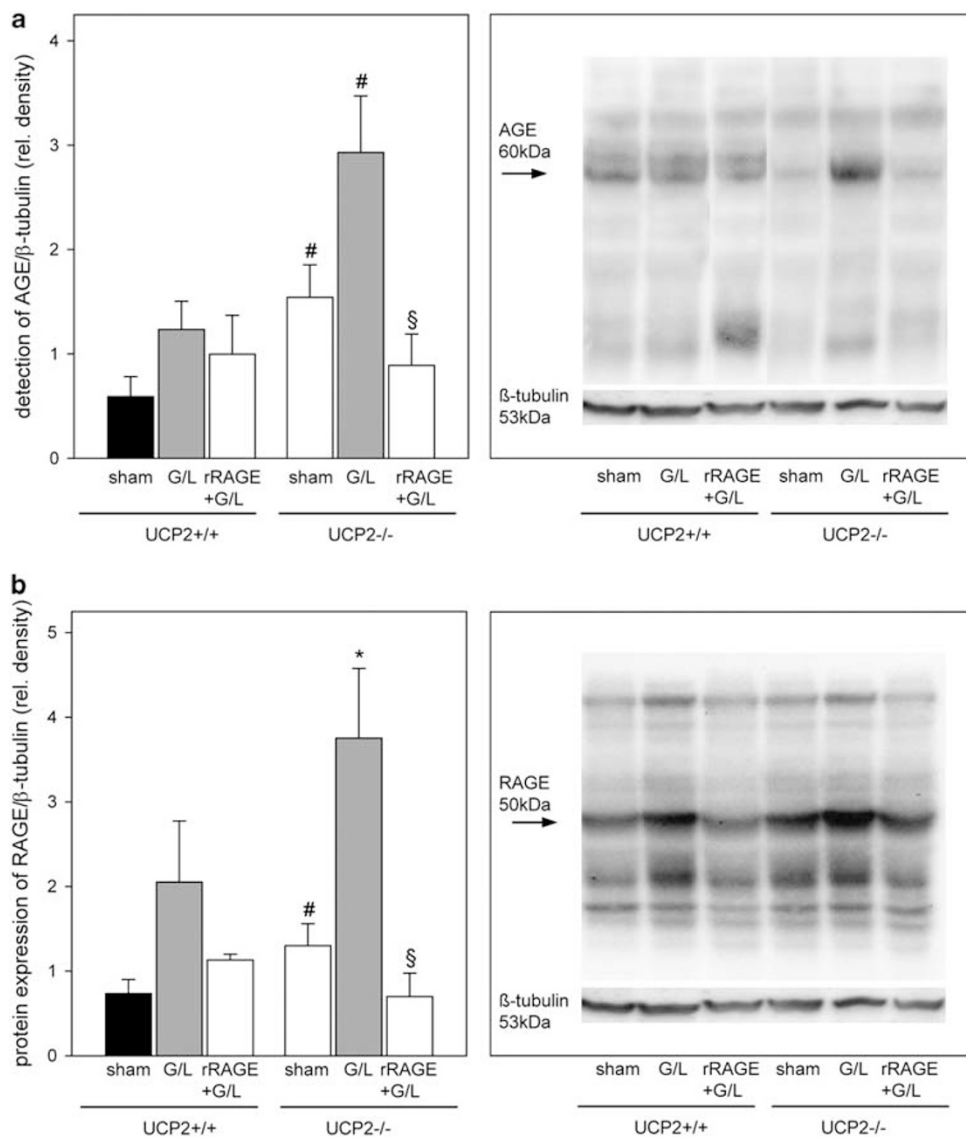


Figure 6 Densitometric analysis and representative western blots of AGE (60 kDa; **a**) and RAGE (50 kDa; **b**) in the livers of UCP2^{+/+} ($n = 21$) and UCP2^{-/-} animals ($n = 21$). Signals were corrected with that of β -tubulin. Animals were injected with either saline (sham; $n = 14$), G/L (720 mg/kg/10 μ g/kg BW i.p.) (G/L; $n = 14$) or recombinant RAGE (10 μ g i.p.; rRAGE + G/L; $n = 14$) at 12 h before G/L challenge. In all animals, analysis was carried out 6 h after G/L exposure. Note the high protein levels of AGE and RAGE in UCP2^{-/-} mice, which could significantly be attenuated by rRAGE pretreatment. Values are given as means \pm s.e.m.; ANOVA, *post hoc* pairwise comparison tests: # $P < 0.05$ vs UCP2^{+/+}; * $P < 0.05$ vs sham; § $P < 0.05$ vs G/L.

It is known that the liver is not only the target organ, but also an important site for clearance and catabolism of circulating AGE. Interestingly, the endocytotic clearance of AGE^{20,49} is reduced in the aging liver because of the pseudocapillarization process of sinusoids with loss of fenestrae and basal lamina formation.²¹ In addition, the detoxification of AGE by the glyoxalase system is described to be age-dependent.¹⁹ Extending this information, we now show that mitochondrial dysfunction in UCP2^{-/-} mice is associated with a decrease of glyoxalase-I activity that in turn may be causative for the increased AGE formation.

In AGE-induced tissue damage and dysfunction, RAGE-dependent mechanisms are likely to be involved.^{50,51} RAGE has been identified as a central signal transduction receptor,

mediating long-lasting NF- κ B activation in various cell types, including mononuclear phagocytes,⁵² and leading to liver tissue injury. In line with this, there is evidence for the involvement of RAGE in many liver diseases.^{33,53-55} Zeng *et al*⁵⁵ could show that RAGE modulates hepatic ischemia/reperfusion injury—at least in part—by activation of a signal cascade linked to proinflammatory and cell death-promoting responses. Further, it is reported that the expression of RAGE is upregulated in many organ lesions,^{25,56} emphasizing the (patho)-physiological role of RAGE in inflammation. Together with the fact that UCP2^{-/-} mice exhibit higher expression of RAGE than UCP2^{+/+} mice, they respond to G/L exposure with significantly higher AST and ALT plasma activities, indicating more pronounced tissue necrosis.

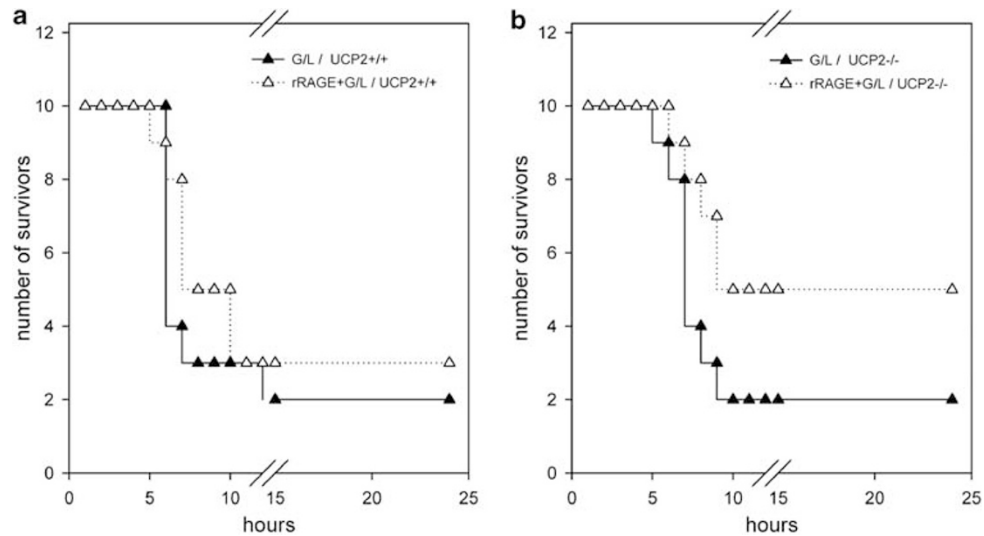


Figure 7 Survival rate of UCP2^{+/+} ($n=20$) (a) and UCP2^{-/-} animals ($n=20$) (b), which were injected with either G/L (720 mg/kg/10 μ g/kg BW i.p.) (G/L; $n=10$ each) or recombinant RAGE (10 μ g i.p.; rRAGE+G/L; $n=10$ each) at 12 h before G/L challenge. Mortality was assessed every 30 min during the first 12 h and thereafter every 4 h until 24 h.

Unexpectedly, however, the more pronounced liver injury in UCP2^{-/-} mice compared with UCP2^{+/+} animals did not further increase mortality rate.

Nevertheless, it is reasonable to state that the mitochondrial dysfunction-associated rise in hepatic AGE and RAGE expression increases vulnerability of the liver to an inflammatory stimulus.⁵⁷ It has been shown that sRAGE and F(ab)₂ fragments to block ligand binding to RAGE are capable of reducing an inflammatory response.^{28,58} Therefore, we used recombinant RAGE, which functions as a decoy by binding RAGE ligands and prevents their interaction with extracellular RAGE by blocking the receptor.²⁸ The almost complete abrogation of necrotic tissue damage in UCP2^{-/-} livers and the better survival rate of G/L-challenged UCP2^{-/-} mice on RAGE blockade underlines that a blockade of RAGE diminishes hepatic vulnerability to inflammation. Interestingly, after the application of rRAGE, liver injury was significantly more reduced in UCP2^{-/-} than in UCP2^{+/+} mice. One explanation is that blockade of RAGE by pretreatment with rRAGE is more efficient in UCP2^{-/-} mice compared with UCP2^{+/+} mice, as indicated by a reduction of hepatic RAGE expression to 14% in UCP2^{-/-} vs 50% in UCP2^{+/+} animals, respectively.

In summary, we show for the first time that mitochondrial dysfunction leads to chronic oxidative stress, as well as marked accumulation of AGE and rise of RAGE expression in liver tissue. This in consequence markedly increases hepatic response to injury. Thus, oxidative stress-dependent AGE/RAGE interaction could represent an ideal target for therapeutic interventions in the diseased liver.

ACKNOWLEDGEMENT

We cordially thank Saleh Ibrahim (Exzellenz-Zentrum Entzündungsmedizin, Forschungsgruppe Immunogenetik, Universitätsklinikum Schleswig-Holstein,

Lübeck) for providing us UCP2 knockout mice, Björn Kuhla (Research Unit Nutritional Physiology 'Oskar Kellner,' Research Institute for the Biology of Farm Animals (FBN), Dummerstorf) for the fruitful discussion and Berit Blendow, Doris Butzlaff, Dorothea Frenz and Maren Nerowski (Institute for Experimental Surgery, University of Rostock) for their excellent technical assistance.

DISCLOSURE/CONFLICT OF INTEREST

The authors declare no conflict of interest.

1. Harman D. Aging: a theory based on free radical and radiation chemistry. *J Gerontol* 1956;11:298–300.
2. Miquel J, Economos AC, Fleming J, *et al*. Mitochondrial role in cell aging. *Exp Gerontol* 1980;15:575–591.
3. Raha S, Robinson BH. Mitochondria, oxygen free radicals, and apoptosis. *Am J Med Genet* 2001;106:62–70.
4. Skulachev VP. Uncoupling: new approaches to an old problem of bioenergetics. *Biochim Biophys Acta* 1998;1363:100–124.
5. Echtay KS, Roussel D, St-Pierre J, *et al*. Superoxide activates mitochondrial uncoupling proteins. *Nature* 2002;415:96–99.
6. Boss O, Hagen T, Lowell BB. Uncoupling proteins 2 and 3: potential regulators of mitochondrial energy metabolism. *Diabetes* 2000;49:143–156.
7. Mattiasson G, Shamloo M, Gido G, *et al*. Uncoupling protein-2 prevents neuronal death and diminishes brain dysfunction after stroke and brain trauma. *Nat Med* 2003;9:1062–1068.
8. Teshima Y, Akao M, Jones SP, *et al*. Uncoupling protein-2 overexpression inhibits mitochondrial death pathway in cardiomyocytes. *Circ Res* 2003;93:192–200.
9. Nègre-Salvayre A, Hirtz C, Carrera G, *et al*. A role for uncoupling protein-2 as a regulator of mitochondrial hydrogen peroxide generation. *FASEB J* 1997;11:809–815.
10. Duval C, Nègre-Salvayre A, Dogilo A, *et al*. Increased reactive oxygen species production with antisense oligonucleotides directed against uncoupling protein 2 in murine endothelial cells. *Biochem Cell Biol* 2002;80:757–764.
11. Brownlee M. Glycation and diabetic complications. *Diabetes (Lilly Lecture, 1994)* 1994;43:836–841.
12. Schmidt A, Kuhla B, Bigl K, *et al*. Cell cycle related signaling in Neuro2a cells proceeds via the receptor for advanced glycation end products. *J Neural Transm* 2007;114:1413–1424.
13. Bucala R, Makita Z, Vega G, *et al*. Modification of low density lipoprotein by advanced glycation end products contributes to the

- dyslipidemia of diabetes and renal insufficiency. *Proc Natl Acad Sci USA* 1994;91:9441–9445.
14. Takeuchi M, Kikuchi S, Sasaki N, *et al*. Involvement of advanced glycation end-products (AGEs) in Alzheimer's disease. *Curr Alzheimer Res* 2004;1:39–46.
 15. Araki N, Ueno N, Chakrabarti B, *et al*. Immunochemical evidence for the presence of advanced glycation end products in human lens proteins and its positive correlation with aging. *J Biol Chem* 1992;267:10211–10214.
 16. Brownlee M. Advanced protein glycosylation in diabetes and aging. *Annu Rev Med* 1995;46:223–234.
 17. Kume S, Takeya M, Mori T, *et al*. Immunohistochemical and ultrastructural detection of advanced glycation end products in atherosclerotic lesions of human aorta with a novel specific monoclonal antibody. *Am J Pathol* 1995;147:654–667.
 18. Thornalley PJ. Glyoxalase I—structure, function and a critical role in the enzymatic defence against glycation. *Biochem Soc Trans* 2003;31:1343–1348.
 19. Kuhla B, Boeck K, Lüth HJ, *et al*. Age-dependent changes of glyoxalase I expression in human brain. *Neurobiol Aging* 2006;27:815–822.
 20. Smedsrød B, Melkko J, Araki N, *et al*. Advanced glycation end products are eliminated by scavenger-receptor-mediated endocytosis in hepatic sinusoidal Kupffer and endothelial cells. *Biochem J* 1997;322:567–573.
 21. Ito Y, Sørensen KK, Bethea NW, *et al*. Age-related changes in the hepatic microcirculation in mice. *Exp Gerontol* 2007;42:789–797.
 22. Neeper M, Schmidt AM, Brett J, *et al*. Cloning and expression of a cell surface receptor for advanced glycosylation end products of proteins. *J Biol Chem* 1992;267:14998–15004.
 23. Schmidt AM, Hori O, Brett J, *et al*. Cellular receptors for advanced glycation end products. Implications for induction of oxidant stress and cellular dysfunction in the pathogenesis of vascular lesions. *Arterioscler Thromb* 1994;14:1521–1528.
 24. Thornalley PJ. Cell activation by glycated proteins. AGE receptors, receptor recognition factors and functional classification of AGEs. *Cell Mol Biol* 1998;44:1013–1023.
 25. Schmidt AM, Yan SD, Yan SF, *et al*. The biology of the receptor for advanced glycation end products and its ligands. *Biochim Biophys Acta* 2000;1498:99–111.
 26. Bierhaus A, Chevion S, Chevion M, *et al*. Advanced glycation end product-induced activation of NF-kappaB is suppressed by alpha-lipoic acid in cultured endothelial cells. *Diabetes* 1997;46:1481–1490.
 27. Stern D, Yan SD, Yan SF, *et al*. Receptor for advanced glycation end products: a multiligand receptor magnifying cell stress in diverse pathologic settings. *Adv Drug Deliv Rev* 2002;54:615–1625.
 28. Park L, Raman KG, Lee KJ, *et al*. Suppression of accelerated diabetic atherosclerosis by the soluble receptor for advanced glycation end products. *Nat Med* 1998;4:1025–1031.
 29. Freudenberg MA, Keppler D, Galanos C. Requirement for lipopolysaccharide-responsive macrophages in galactosamine-induced sensitization to endotoxin. *Infect Immun* 1986;51:891–895.
 30. Arsenijevic D, Onuma H, Pecqueur C, *et al*. Disruption of the uncoupling protein-2 gene in mice reveals a role in immunity and reactive oxygen species production. *Nat Genet* 2000;26:435–439.
 31. Eipel C, Kidess E, Abshagen K, *et al*. Antileukoproteinase protects against hepatic inflammation, but not apoptosis in the response of D-galactosamine-sensitized mice to lipopolysaccharide. *Br J Pharmacol* 2007;151:406–413.
 32. Kuhla A, Eipel C, Siebert N, *et al*. Hepatocellular apoptosis is mediated by TNFalpha-dependent Fas/FasLigand cytotoxicity in a murine model of acute liver failure. *Apoptosis* 2008;13:1427–1438.
 33. Cataldegirmen G, Zeng S, Feirt N, *et al*. RAGE limits regeneration after massive liver injury by coordinated suppression of TNF-alpha and NF-kappaB. *J Exp Med* 2005;201:473–484.
 34. Wautier JL, Zoukourian C, Chappey O, *et al*. Receptor-mediated endothelial cell dysfunction in diabetic vasculopathy. Soluble receptor for advanced glycation end products blocks hyperpermeability in diabetic rats. *J Clin Invest* 1996;97:238–243.
 35. Allen RE, Lo TW, Thornalley PJ. Purification and characterisation of glyoxalase II from human red blood cells. *Eur J Biochem* 1993;213:1261–1267.
 36. Horiuchi S, Araki N, Morino Y. Immunochemical approach to characterize advanced glycation end products of the Maillard reaction. Evidence for the presence of a common structure. *J Biol Chem* 1991;266:7329–7332.
 37. Ghavami S, Rashedi I, Dattilo BM, *et al*. S100A8/A9 at low concentration promotes tumor cell growth via RAGE ligation and MAP kinase-dependent pathway. *J Leukoc Biol* 2008;83:1484–1492.
 38. Miyata T, Taneda S, Kawai R, *et al*. Identification of pentosidine as a native structure for advanced glycation end products in beta-2-microglobulin-containing amyloid fibrils in patients with dialysis-related amyloidosis. *Proc Natl Acad Sci USA* 1996;93:2353–2358.
 39. Sastre J, Pallardó FV, Plá R, *et al*. Aging of the liver: age-associated mitochondrial damage in intact hepatocytes. *Hepatology* 1996;24:1199–1205.
 40. Rolo AP, Palmeira CM. Diabetes and mitochondrial function: role of hyperglycemia and oxidative stress. *Toxicol Appl Pharmacol* 2006;212:167–178.
 41. Chagnon P, Bétard C, Robitaille Y, *et al*. Distribution of brain cytochrome oxidase activity in various neurodegenerative diseases. *Neuroreport* 1995;6:711–715.
 42. Beckman KB, Ames BN. The free radical theory of aging matures. *Physiol Rev* 1998;78:547–581.
 43. Navarro A, Boveris A. The mitochondrial energy transduction system and the aging process. *Am J Physiol Cell Physiol* 2007;292:C670–C686.
 44. Basta G, Schmidt AM, De Caterina R. Advanced glycation end products and vascular inflammation: implications for accelerated atherosclerosis in diabetes. *Cardiovasc Res* 2004;63:582–592.
 45. Cooper ME. Importance of advanced glycation end products in diabetes-associated cardiovascular and renal disease. *Am J Hypertens* 2004;17:315–385.
 46. Stitt AW, Frizzell N, Thorpe SR. Advanced glycation and advanced lipoxidation: possible role in initiation and progression of diabetic retinopathy. *Curr Pharm Des* 2004;10:3349–3360.
 47. Sebeková K, Kupcová V, Schinzel R, *et al*. Markedly elevated levels of plasma advanced glycation end products in patients with liver cirrhosis—amelioration by liver transplantation. *J Hepatol* 2002;36:66–71.
 48. Stolzing A, Widmer R, Jung T, *et al*. Degradation of glycated bovine serum albumin in microglial cells. *Free Radic Biol Med* 2006;40:1017–1027.
 49. Takata K, Horiuchi S, Araki N, *et al*. Endocytic uptake of nonenzymatically glycosylated proteins is mediated by a scavenger receptor for aldehyde-modified proteins. *J Biol Chem* 1988;263:14819–14825.
 50. Yamagishi S, Hsu CC, Taniguchi M, *et al*. Receptor-mediated toxicity to pericytes of advanced glycosylation end products: a possible mechanism of pericyte loss in diabetic microangiopathy. *Biochem Biophys Res Commun* 1995;213:681–687.
 51. Tsuji H, Iehara N, Masegi T, *et al*. Ribozyme targeting of receptor for advanced glycation end products in mouse mesangial cells. *Biochem Biophys Res Commun* 1998;245:583–588.
 52. Liliensiek B, Weigand MA, Bierhaus A, *et al*. Receptor for advanced glycation end products (RAGE) regulates sepsis but not the adaptive immune response. *J Clin Invest* 2004;113:1641–1650.
 53. Hiwatashi K, Ueno S, Abeyama K, *et al*. A novel function of the receptor for advanced glycation end-products (RAGE) in association with tumorigenesis and tumor differentiation of HCC. *Ann Surg Oncol* 2008;15:923–933.
 54. Ekong U, Zeng S, Dun H, *et al*. Blockade of the receptor for advanced glycation end products attenuates acetaminophen-induced hepatotoxicity in mice. *J Gastroenterol Hepatol* 2006;21:682–688.
 55. Zeng S, Feirt N, Goldstein M, *et al*. Blockade of receptor for advanced glycation end product (RAGE) attenuates ischemia and reperfusion injury to the liver in mice. *Hepatology* 2004;39:422–432.
 56. Basta G, Lazzarini G, Massaro M, *et al*. Advanced glycation end products activate endothelium through signal-transduction receptor RAGE: a mechanism for amplification of inflammatory responses. *Circulation* 2002;105:816–822.
 57. De la Fuente M. Role of neuroimmunomodulation in aging. *Neuroimmunomodulation* 2008;15:213–223.
 58. Taguchi A, Blood DC, del Toro G, *et al*. Blockade of RAGE-amphoterin signalling suppresses tumour growth and metastases. *Nature* 2000;405:354–360.